

Osteogenicity and bone re-growth induced by an innovative collagen/hydroxylapatite hybrid scaffold: in vitro and in vivo studies

Dr ssa Elisa Mazzoni, PhD, CRA



1. Osteoconductivity of Complex Biomaterials Assayed by Fluorescent-Engineered Osteoblast-like Cells

Marco Manfrini · Elisa Mazzoni · Giovanni Barbanti-Brodano ·
Pierfrancesco Nocini · Antonio D'agostino ·
Leonardo Trombelli · Mauro Tognon

Biomaterials employed for the bone regeneration
can be assayed for specific features
such as osteoconductivity.



In this study, the composite HA88%/collagen
9,5%/chondroitin-sulfate 2,5% biomaterial (Biostite)
was investigated using an engineered human cell line,
named Saos-eGFP

Cell morphology, markers, spreading, and proliferation on orthopaedic biomaterials. An innovative cellular model for the "in vitro" study

Cristina Morelli,¹ Giovanni Barbanti-Brodano,² Alessandra Ciannilli,¹ Katia Campioni,¹ Stefano Boriani,² Mauro Tognon¹

¹Department of Morphology and Embryology, Center of Biotechnology, University of Ferrara, Ferrara, Italy
²Ortopedia e Traumatologia-Chirurgia del Rachide, Ospedale Maggiore "C.A. Pizzardi", AUSL Bologna, Italy

Received 2 August 2005; revised 9 December 2006; accepted 2 January 2007
Published online 27 March 2007 in Wiley InterScience (www.interscience.wiley.com). DOI: 10.1002/jbm.a.31262

Abstract: The aims of tissue engineering are the *in vitro* reconstruction of functionally active tissues, and the *in vivo* induction of their appropriate development. The great progresses in the fields of biology and biomaterials represent key events, which allowed the recent improvement of tissue engineering. In the orthopaedic perspective, tissue engineering is focused on the development of innovative materials, whose action consists in recruiting bone progenitor cells and in stimulating their proliferation. In this context, it should remind that these materials should not only allow cells adhesion and proliferation, but also ensure that attached cells maintain the cellular properties of the original tissue. In this study, a new cellular model, suitable for the rapid *in vitro* determination of the above parameters, is

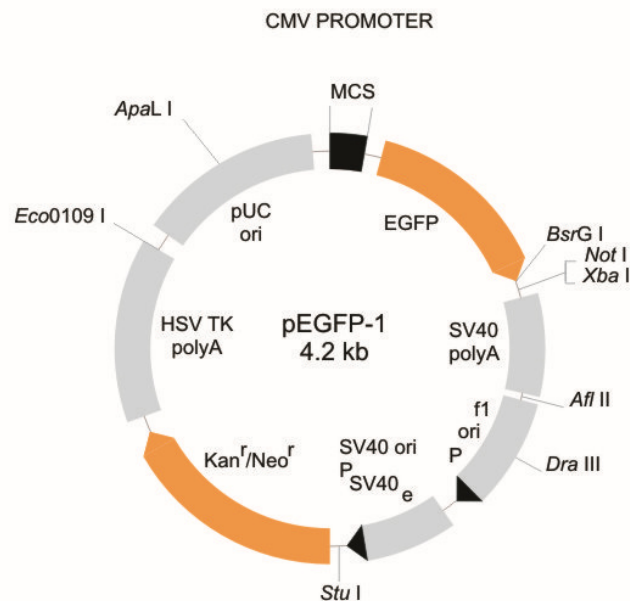
presented. The cell model derives from a human osteosarcoma cell line, Saos-2, which maintained the cytological features of the osteoblast cells. The cell line was genetically modified to express constitutively the enhanced green fluorescent protein. The engineered cell line Saos-eGFP represents a suitable *in vitro* mode for studying the biocompatibility, the cell adhesion, spreading, and proliferation on biomaterials developed for clinical applications. © 2007 Wiley Periodicals, Inc. *J Biomed Mater Res* 83A: 178–183, 2007

Key words: engineered cell; enhanced green fluorescent protein; osteoblast molecular marker; pre-clinical characterization

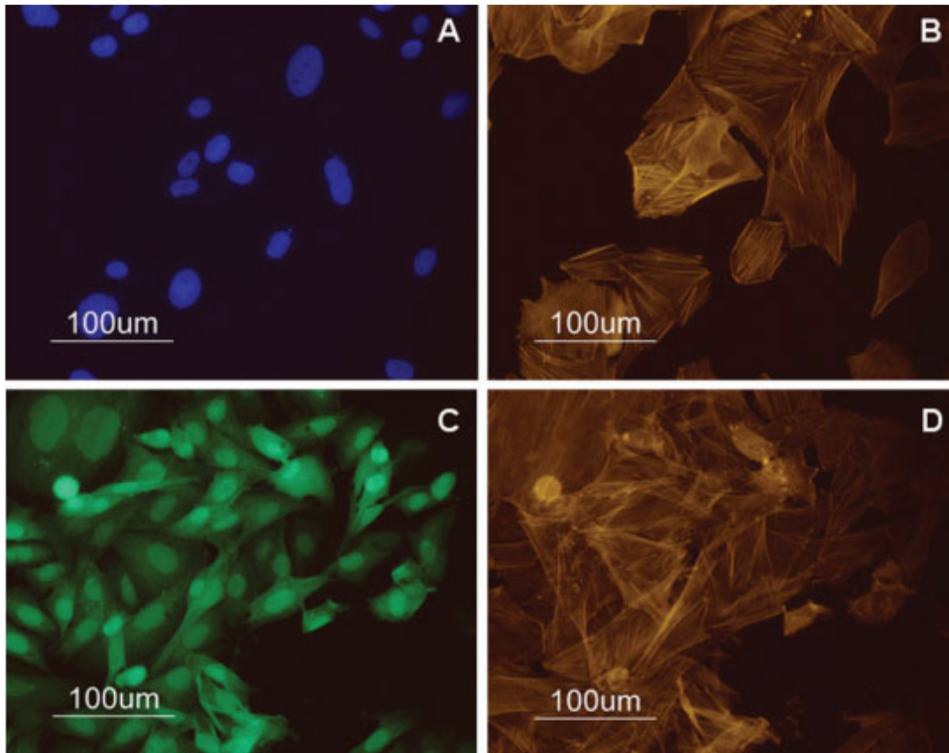
INTRODUCTION

The possibility of either regenerating *in vitro* func-

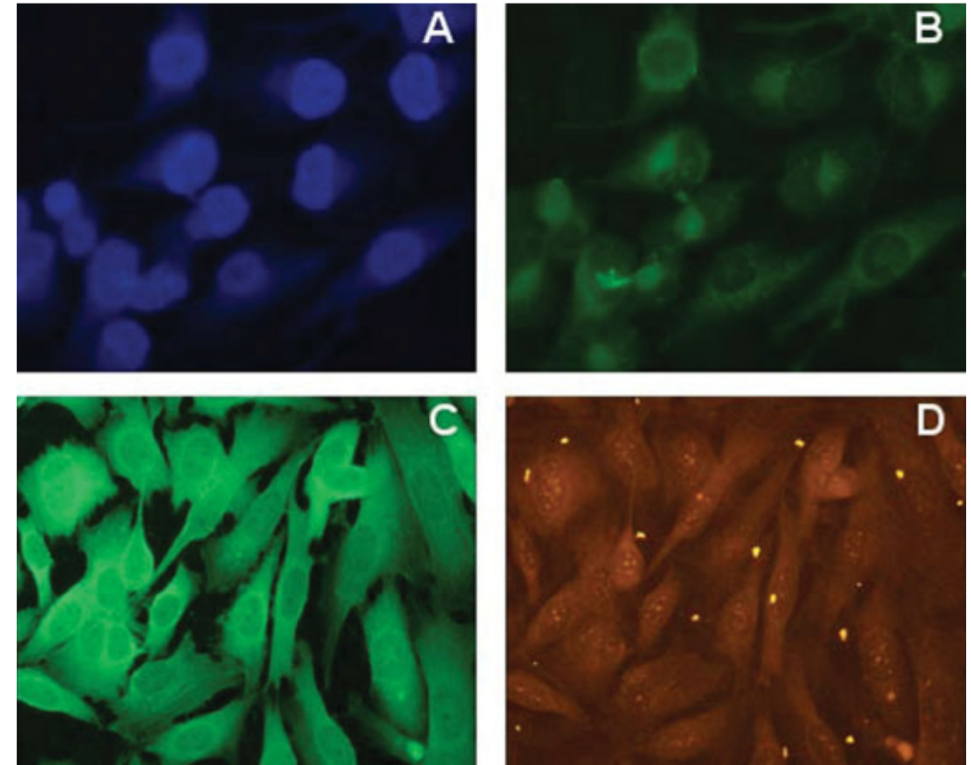
kinds of bone fractures/defects or to achieve a solid spine fusion after a surgical arthrodesis, often implies for patients a long time of inactivity or hos-



Saos-eGFP

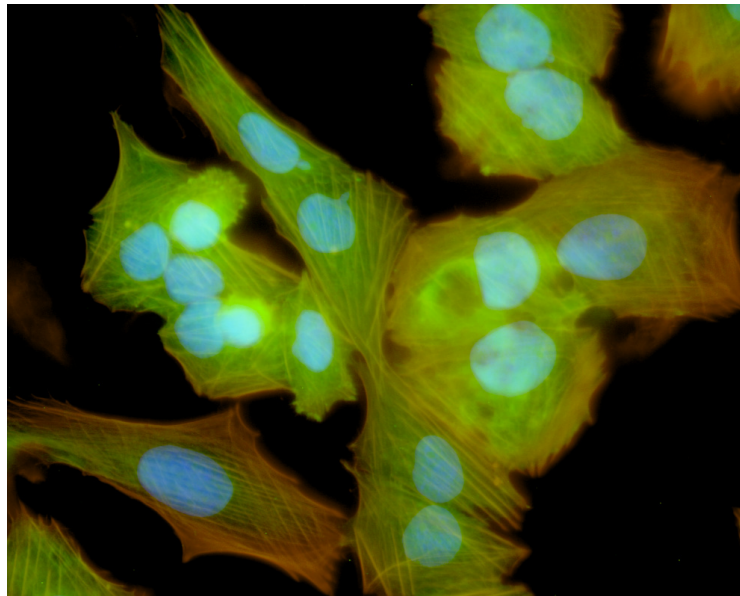
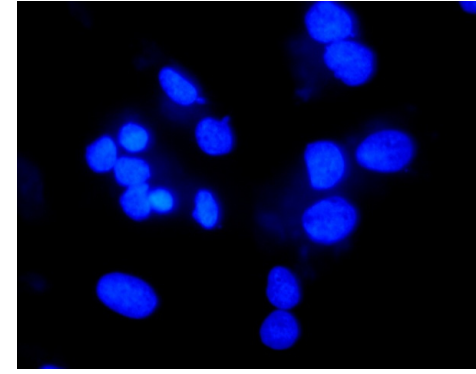
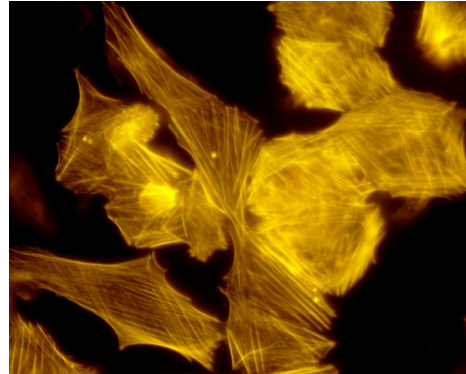
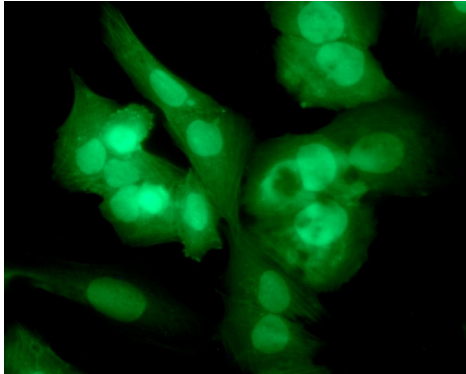


Fluorescence micrographs showing the actin fibres architecture in Saos-eGFP (D) and in the parental Saos-2 (B) cells. The nuclei of Saos-2 cells (A) were counterstained with DAPI (40-6-diamidino-2-phenylindole), while Saos-eGFP cells (C) were directly visualized because of their constitutive green fluorescence.

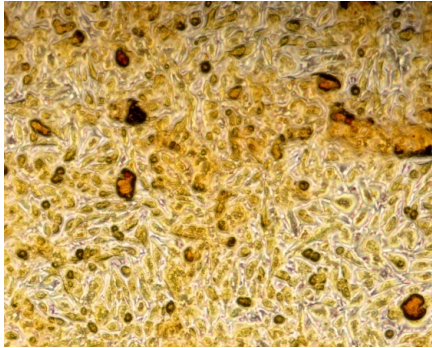


Fluorescence micrographs showing the distribution of osteopontin in Saos-2 (B) and Saos-eGFP (D) cells. The nuclei of Saos-2 cells (A) were counterstained with DAPI (40-6-diamidino-2-phenylindole), while Saos-eGFP cells (C) were directly visualized with the UV light microscopy because of their constitutive green fluorescence.

Phalloidin TRITC

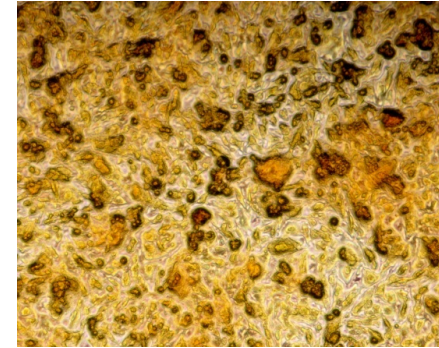


Alizarina Red

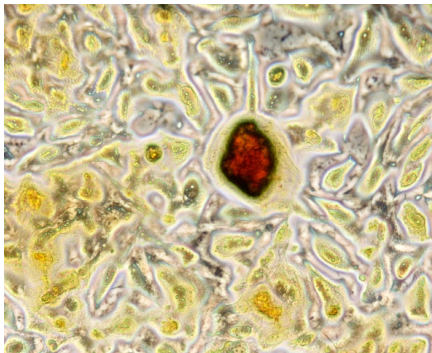


Ingrandimento 10x

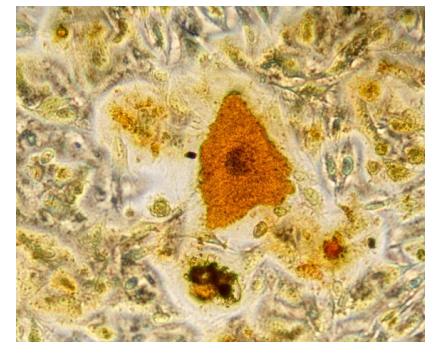
250000 cellule/cm²



400000 cellule/cm²

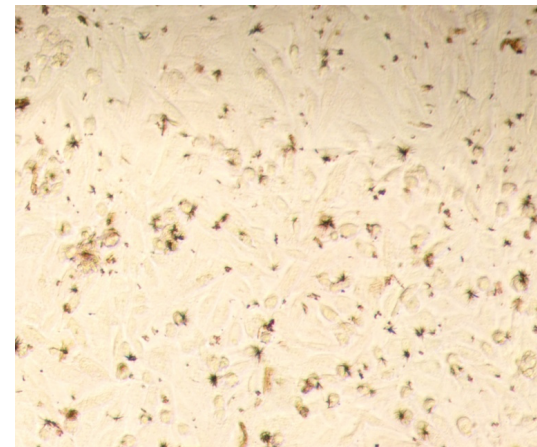
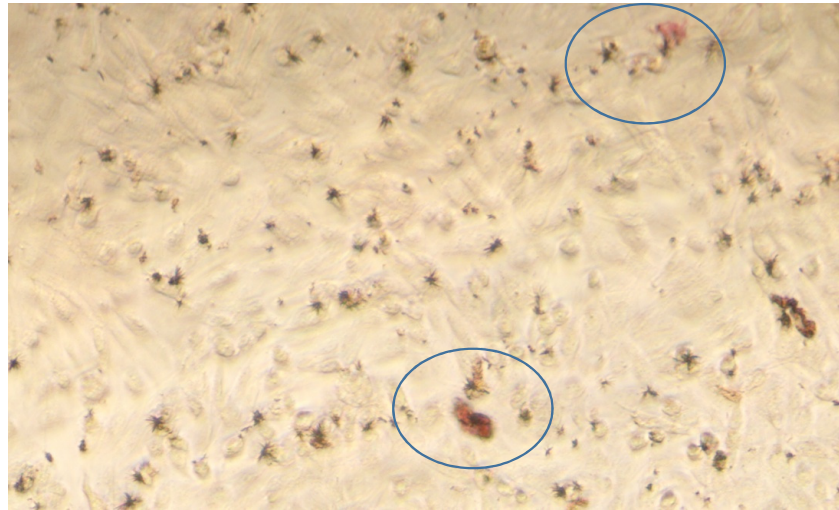


Ingrandimento 20x



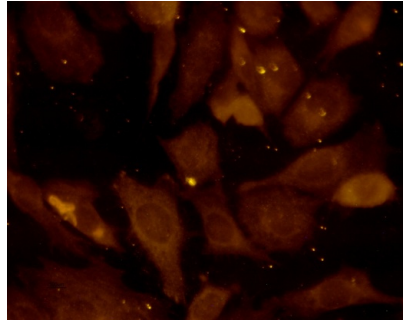
MeOH/acetic acid solution

Alkaline phosphatase staining

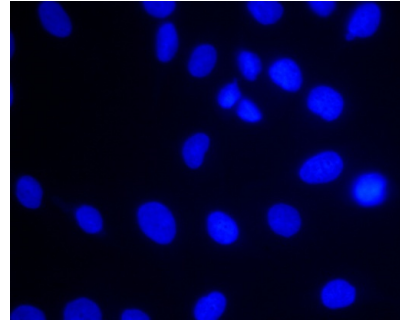


Alkaline Phosphatase Detection Kit

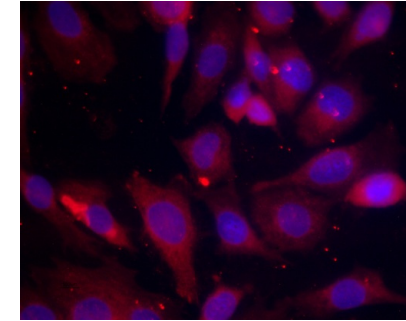
Immunofluorescence



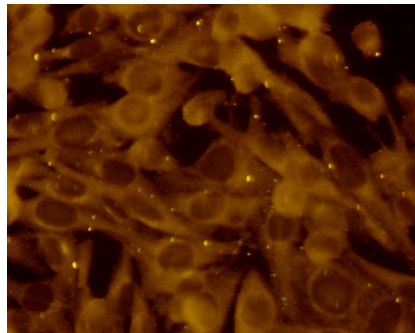
CLEC 3B Ab I 1:50



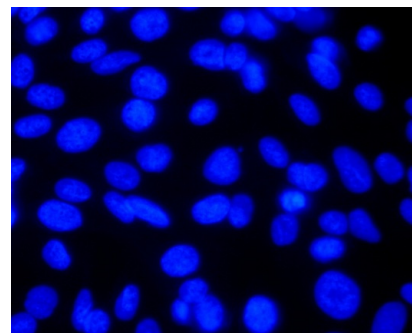
DAPI



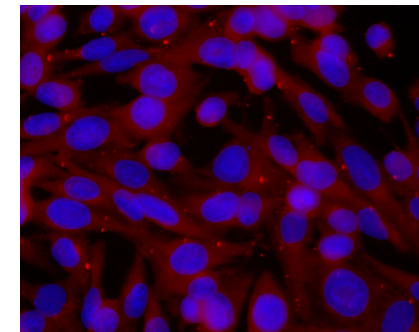
CLEC 3B merge



SPP1 Ab1 1:100



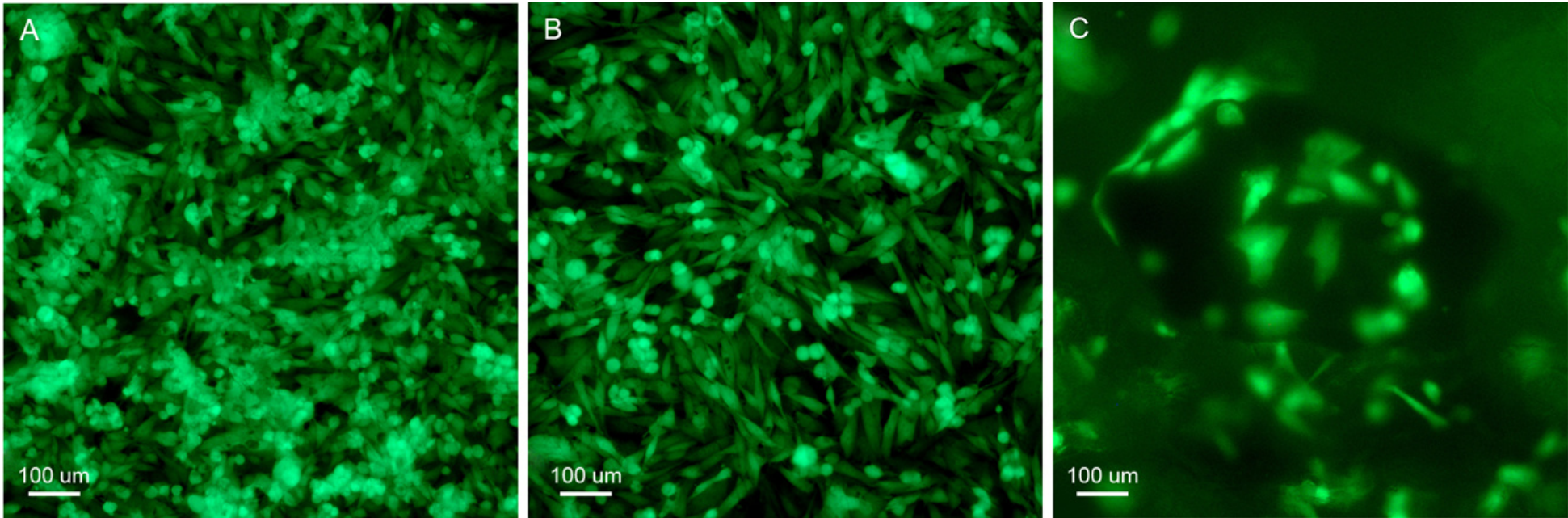
DAPI



SPP1 merge

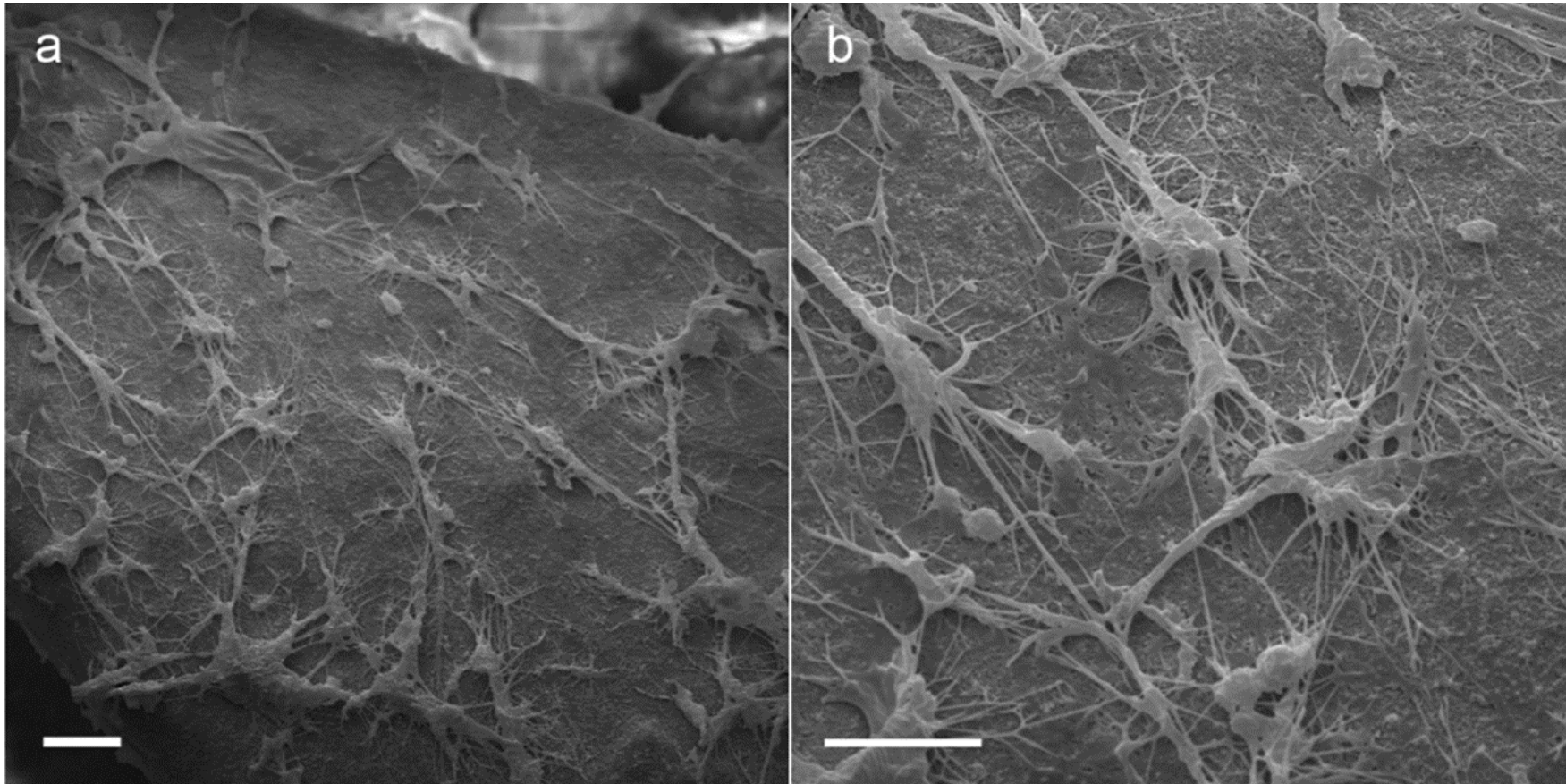
Ab II (anti-mouse IgG TRITC) 1:100

Cell Adhesion and Proliferation Assays



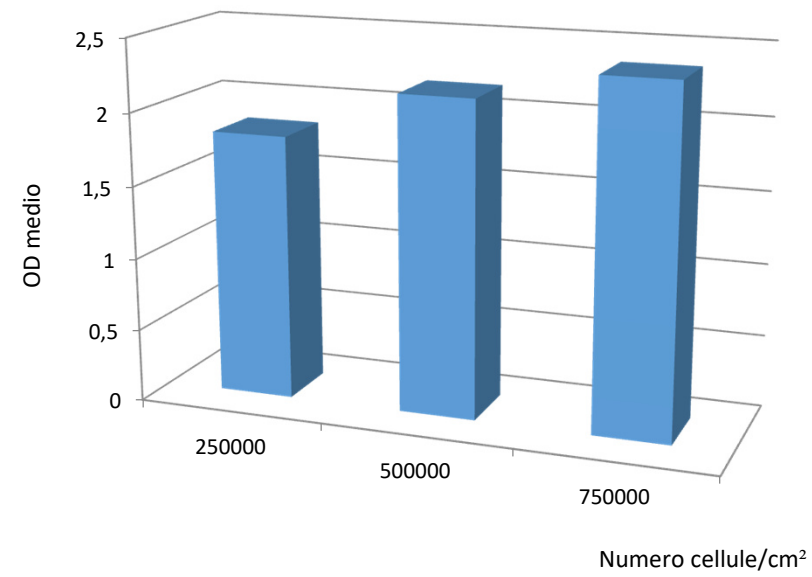
We showed that the Saos-eGFP cellular model is suitable for in vitro biomaterial assays, and more specifically for assessing osteoconductivity.

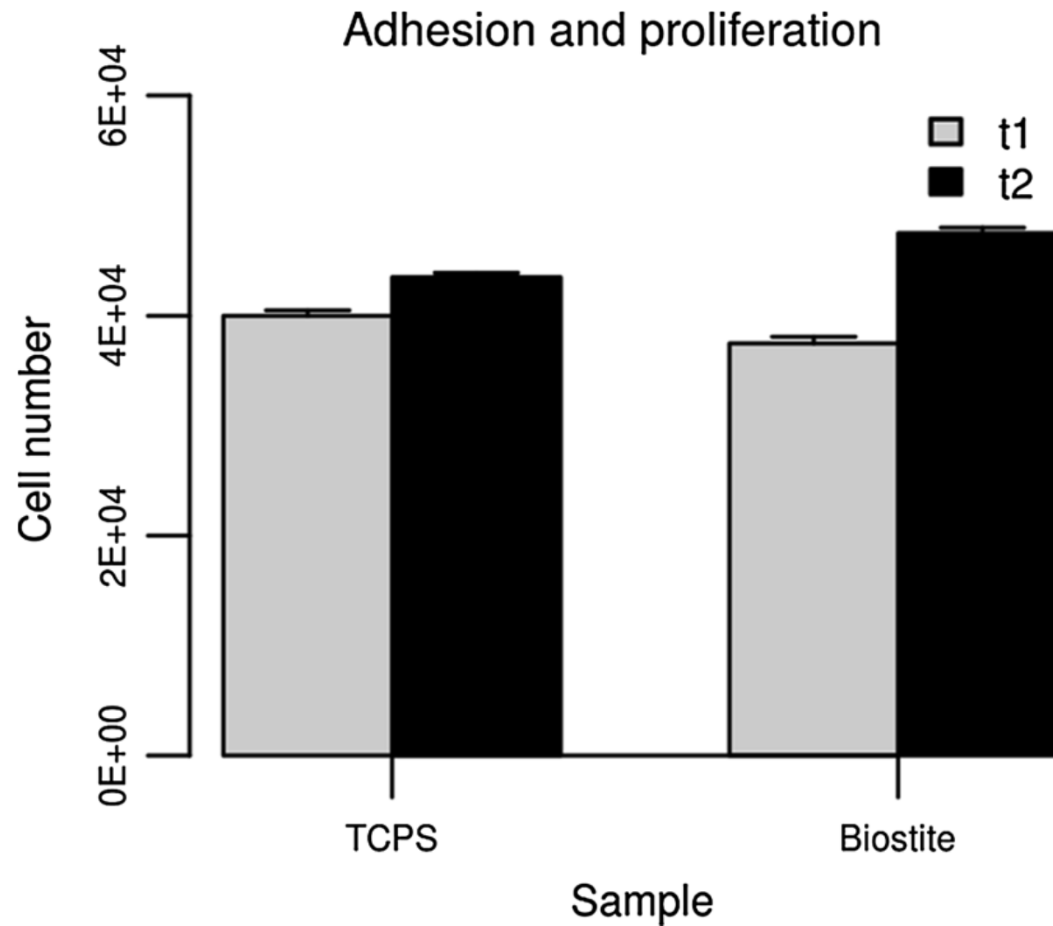
SEM analysis



SEM analysis of the cell morphology and distribution on the scaffold after 96 h of incubation. Cells were homogeneously spread on the substrate, exhibited cytoplasmic bridges and their morphology did not show any sort of alteration. Magnification a 1,000x; b 3,000x; scale bar = 20 μ m

Alamar Blue





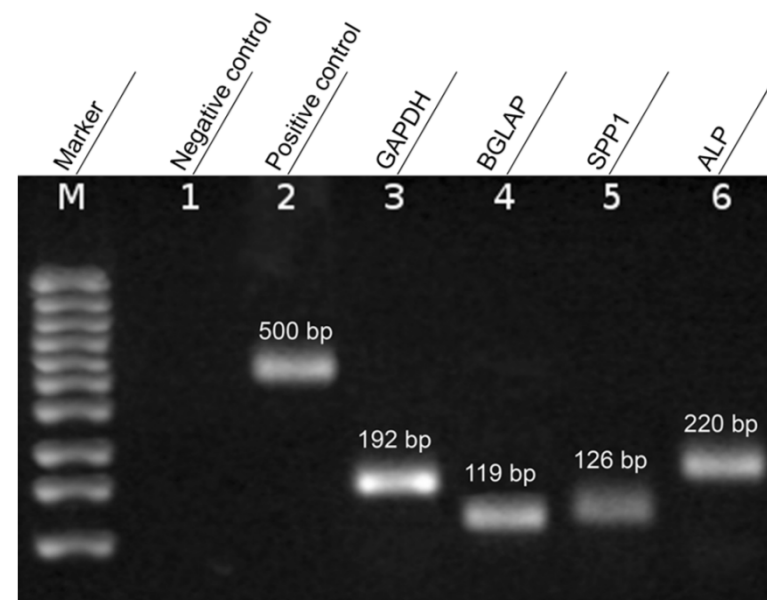
Adhesion and proliferation of Saos-eGFP grown on the scaffold and control. Counts read at 24 and 96 h of incubation. Values were obtained from interpolation with the calibration curve. Fluorescence values are expressed as mean \pm SD. Sample = scaffold, TCPS = plastic control

Gene Expression Analysis of Osteogenic Molecular Markers

Table 1 RT-PCR assay primers

Gene name	Ensembl gene identifier	Sequence	Pos	Len	Tm	Amp (bp)
GAPDH	ENSG00000111640	F: 5'-GTCAACGGATTTGGTC-3'	687	16	55.7	192
		R: 5'-TTCCATTGATGACAAGC-3'	879	17	55.4	
BGLAP	ENSG00000242252	F: 5'-TATCAATGGCTGGGAG-3'	429	16	55.6	119
		R: 5'-ATAGCCTCCTGAAAG-3'	548	16	55.0	
SPP1	ENSG00000118785	F: 5'-AACAAGAGACCCTTCC-3'	373	16	55.7	126
		R: 5'-TCTACATCATCAGAGTCG-3'	499	18	55.9	
ALP	ENSG00000162551	F: 5'-AGTGCCAGAGAAAGAG-3'	303	16	55.8	220
		R: 5'-ACTTGTCATCTCCAG-3'	523	16	55.4	

Gene name, Ensembl identifier, forward (F) and reverse (R) primer sequences, cDNA primer pairing position (Pos), primer length (Len), melting temperature (Tm) and amplicon length (Amp)



The development of an engineered cell line derived from human bone precursor cells constitutively expressing a fluorescent protein during growth and differentiation, may provide an excellent cellular model to be employed to assay scaffolds, because it closely resembles the *in vivo* physiological conditions



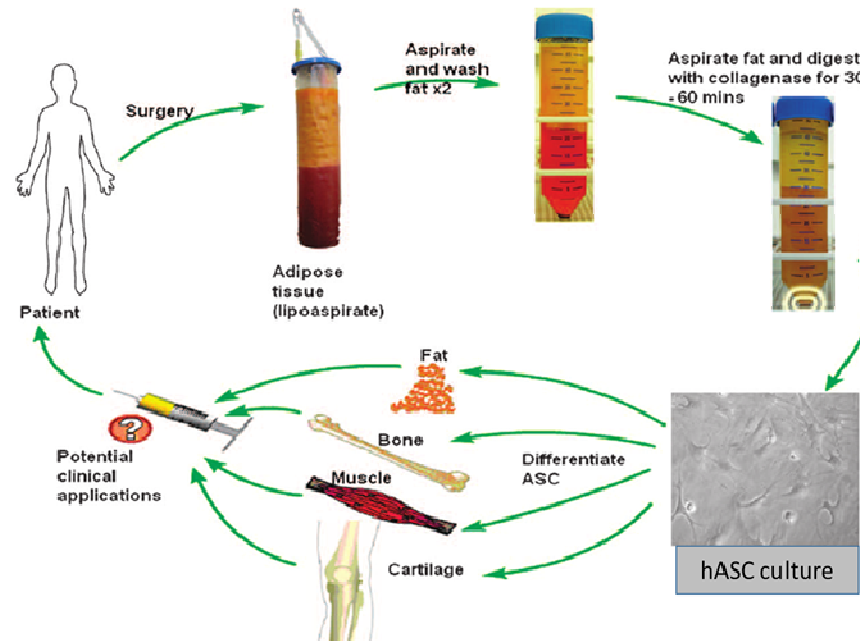
II-III. Osteogenicity and bone re-growth induced by an innovative collagen/hydroxylapatite hybrid scaffold: in vitro and in vivo studies



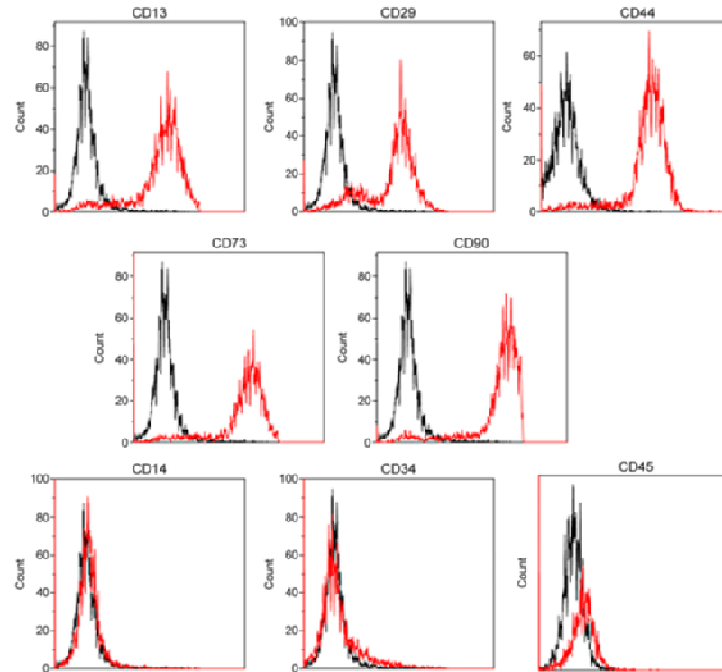
Human adipose stem cells induced to osteogenic differentiation by an innovative collagen/hydroxylapatite hybrid scaffold

Elisa Mazzoni,^{*,†,1} Antonio D'Agostino,^{†,1} Marco Manfrini,^{*,‡} Stefania Maniero,^{*} Andrea Puozzo,^{*} Elena Bassi,^{*,§} Stefano Marsico,^{*} Cinzia Fortini,[†] Lorenzo Trevisiol,[†] Simone Patergnani,^{*} and Mauro Tognon^{*,2}

^{*}Department of Morphology, Surgery, and Experimental Medicine, and [†]Department of Medical Sciences, University of Ferrara, Ferrara, Italy; [‡]Department of Surgery, University of Verona, Verona, Italy; [§]Department of Experimental, Diagnostic, and Specialty Medicine, University of Bologna, Bologna, Italy; and ²Section of Anatomical Pathology, University of Parma, Parma, Italy



hASC flow cytometry markers of stem cells

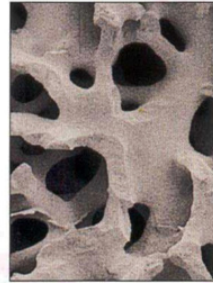


Surface antigenic profile of hASCs that were obtained from adipose tissue from abdominal subcutaneous fat. In the analyzed samples, the level of hASC purity was .95% toward the expression of CD13, -44, -73, and -90, whereas the expression of CD29 was .90%. Phenotypical analysis confirmed that cells were negative for hematopoietic (CD34 and -45) and macrophage (CD14) markers.

Pro Osteon



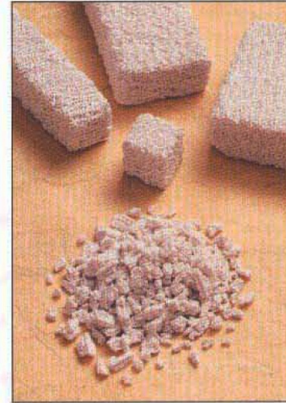
SEM of Human Cancellous Bone



SEM of Pro Osteon Implant 500

LIKE CANCELLOUS BONE, PRO OSTEON LEAVES PLENTY OF ROOM FOR GROWTH.

Harvested from marine coral exoskeletons that are hydrothermally converted to hydroxyapatite, Pro Osteon Implant 500 offers an interconnected porous structure that mimics the porosity of human cancellous bone. The cancellous-like implant provides a matrix for new bone ingrowth and offers structural rigidity during the healing process.



READILY AVAILABLE IN STERILE BLOCKS OR GRANULES.

Pro Osteon is available in a variety of sterile block sizes that are easily cut and shaped to fit the fracture defect, or sterile granules that allow you to literally “pour” the implant into place. Either selection provides a safe, cost-effective alternative to autogenous bone grafts or cadaver bone.

Experimental Design II

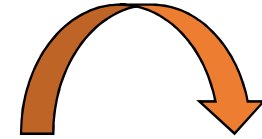
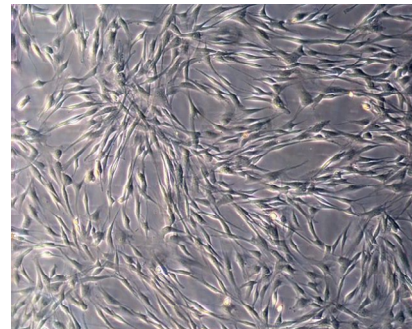
ProOsteon® 200



Scaffold



hASC



Time Course
(T1) 3 days
(T2) 9 days
(T3) 21 days
(T4) 40 days

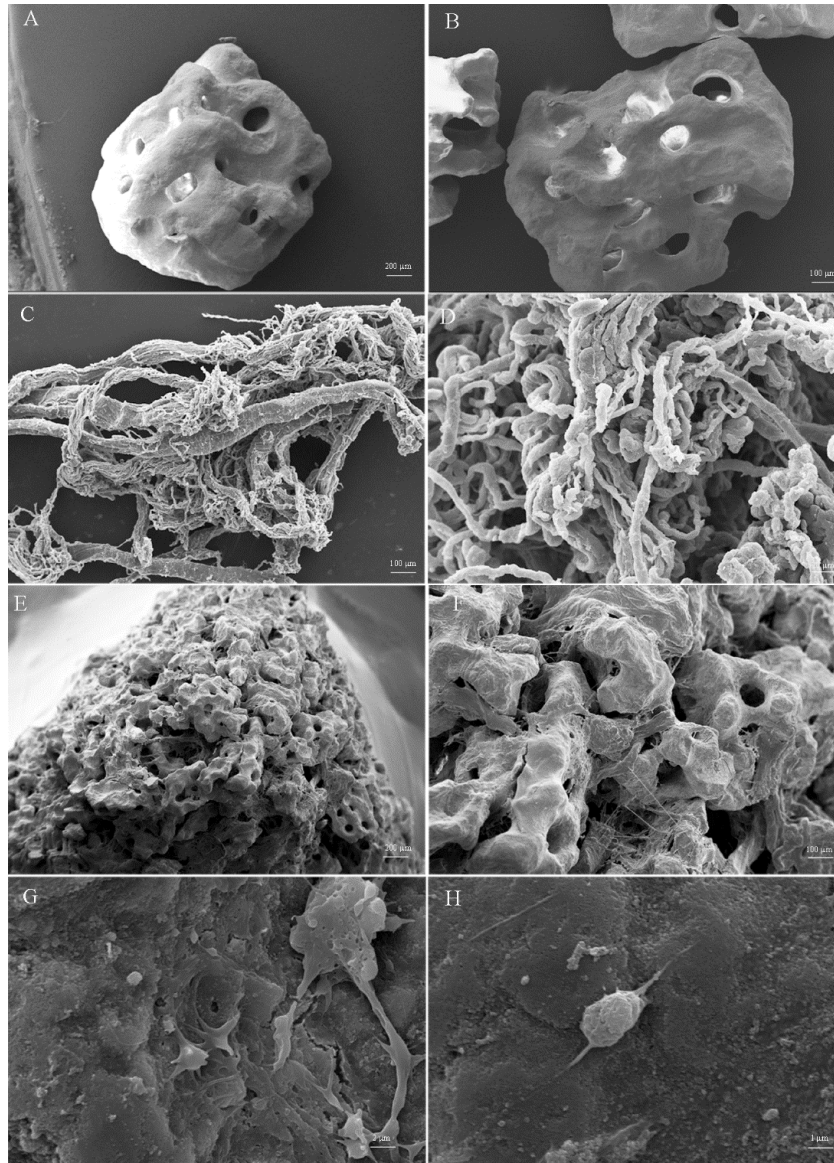


Collagen
(Avitene™)

Experimental groups:

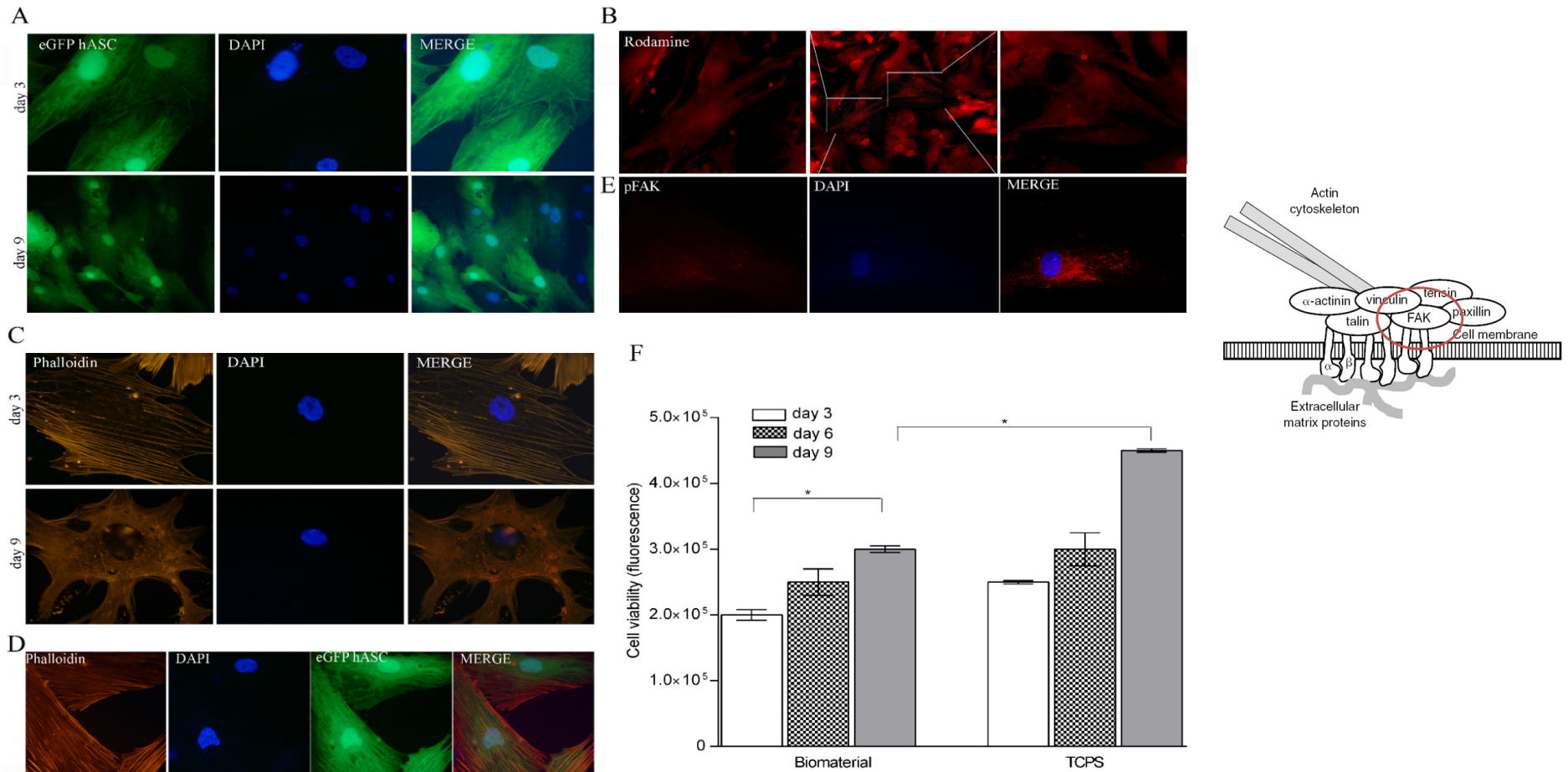
- (i)hASC in well (TCPS)
- (ii)hASC in osteogenic condition (OC) β -glycerol phosphate, ascorbate-2-Phosphate, dexamethason
- (iii)hASC with scaffold

SEM analyses of stem cells and biomaterials



SEM analysis of Coll/Pro Oston200. A, B) Granular Pro Oston 200 coralline HA showed the porous structure with several pores with a range of 190–230 μm. X 3160 (A), X3200 (B). C, D) Organization and structure of collagen fibrils bovine from Avitene Microfibrillar Collagen Hemostat. Fibrils show substantial interweaving and tapered and rounded collagen fibril ends are visible, X3250 (C), X32000 (D). E, F) Coll/ Pro X360 (E), X3181 (F). G, H) SEM analysis of the cell morphology and distribution on scaffold after 3 d of incubation. Cells were homogeneously spread on the substrate, exhibited cytoplasmic bridges, and their morphology did not show any sort of alteration. X 310,000 (G), X315,000 (H).

Cell viability, proliferation, and cytoskeleton architecture



Stem cell viability and cytoskeleton architecture assays. A) hASCs expressing green fluorescence. B) Representative images of culture seeding with biomaterial for 9 d of staining with rhodamine-B obtained with confocal microscope. C) Cytoskeleton analysis by phalloidin TRITC (tetramethylrhodamine isothiocyanate) staining of hASCs that were cultured with biomaterial. (X340). D) Cytoskeleton analysis by phalloidin TRITC staining of hASCs that express eGFP grown with biomaterial. E) Immunostaining with Ab against phosphorylated FAK protein (FAK^{Tyr397}) at d 9 (original magnification, 340). F) hASC metabolic activity measured by colorimetric intensity at d 3, 6, and 9. Granular biomaterial exhibited the highest value in cell viability between d 3 and 9. Statistically significant differences are evident between TCPS and Coll/Pro Osteon200 at d 9.

RT² Profiler PCR Arrays

For pathway-focused gene expression analysis

Figure 2. RT² Profiler PCR Array workflow. Starting from cell, tissue, blood, formalin-fixed paraffin-embedded (FFPE), or laser-capture microdissection (LCM) samples, a comprehensive gene expression profile for your pathway of interest can be achieved in less than 3 hours.

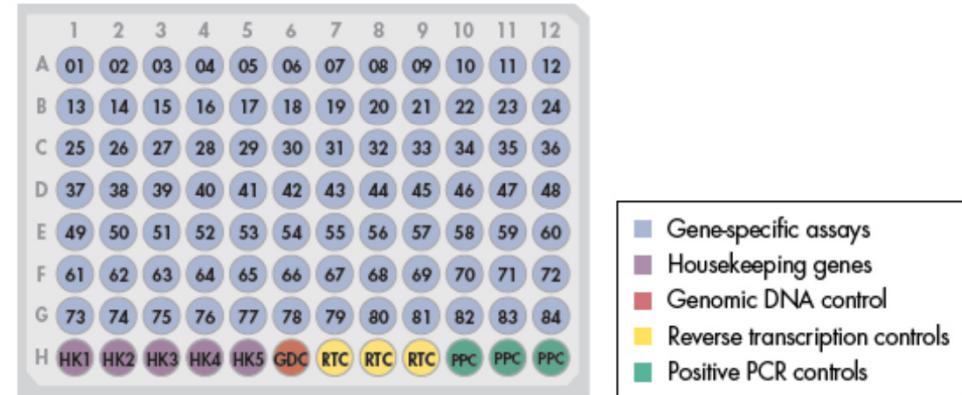
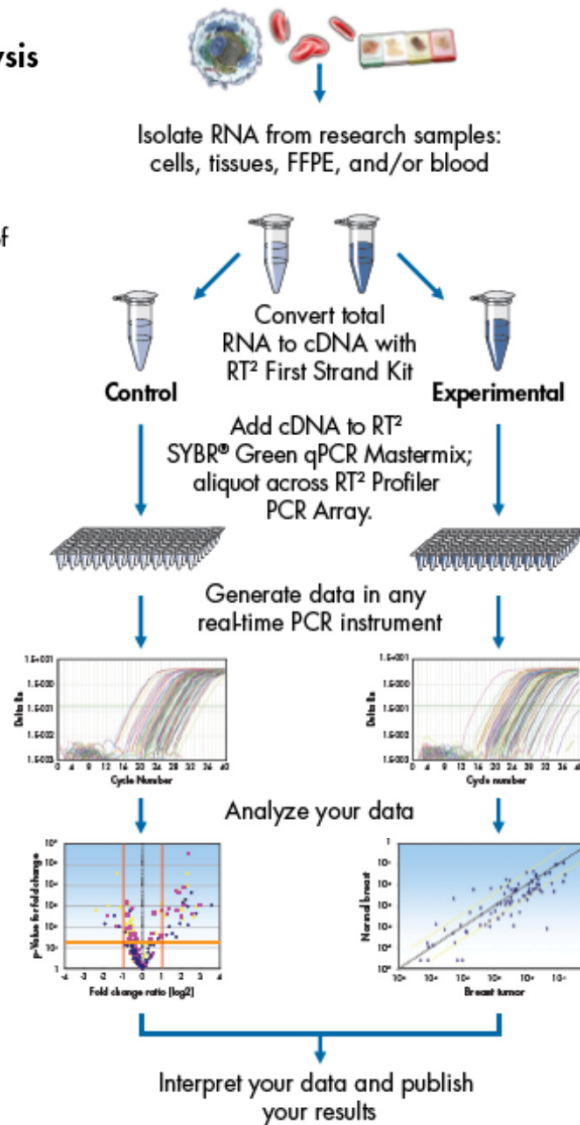
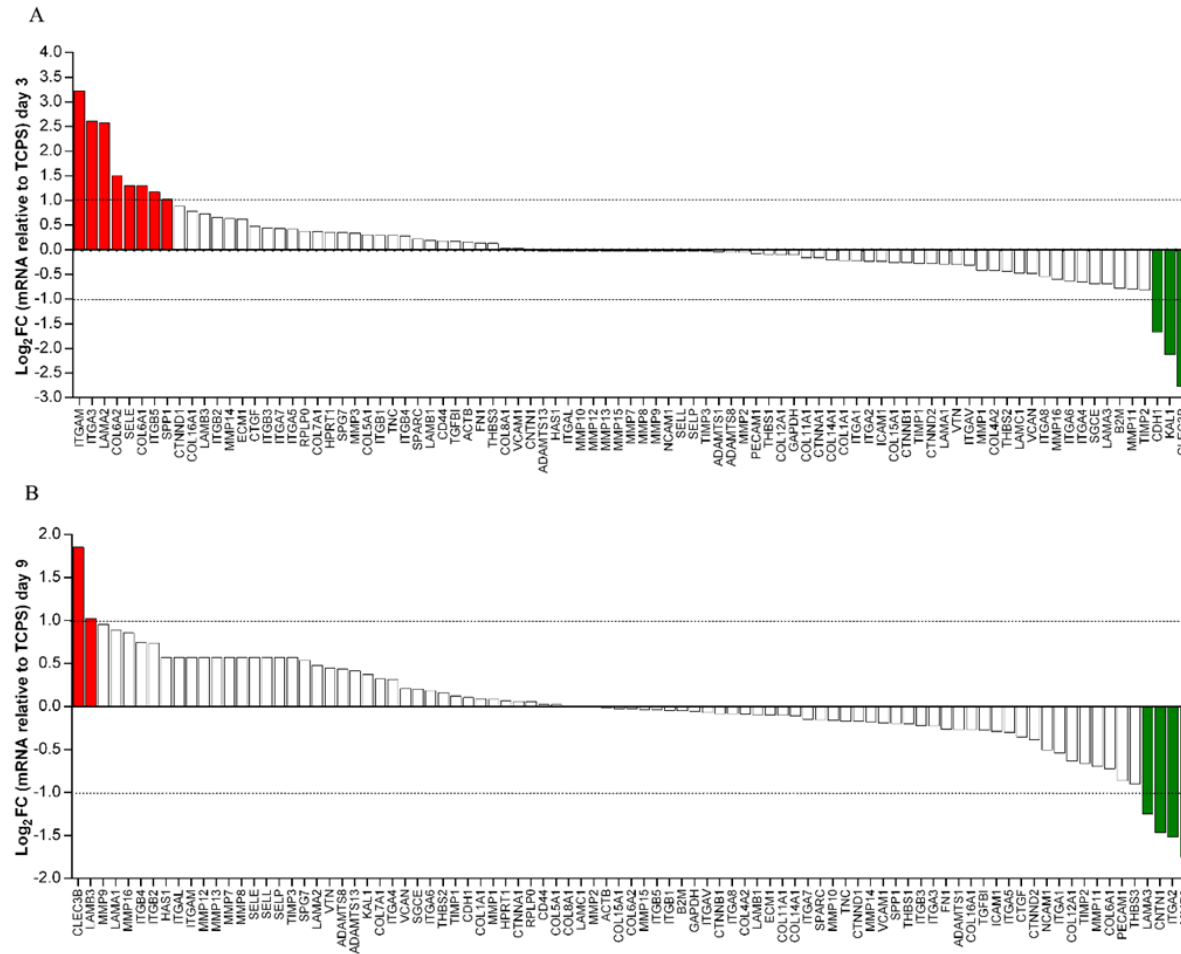


Figure 1. Each well in an RT² Profiler PCR Array measures the relative expression of a gene related to a pathway or disease state. Arrays are available in 4 formats: the 96-well plate, the 384-well plate, the 100-well disc, and the 96x96 chip. Every format includes comprehensive, proprietary controls in addition to the laboratory-verified gene assays, including controls to monitor genomic DNA contamination (GDC), first strand synthesis (RTC), and real-time PCR efficiency (PPC).

[RT² Profiler™ PCR Array Extracellular Matrix and Adhesion Molecules](#)

[RT² Profiler™ PCR Array Human Osteogenesis](#)

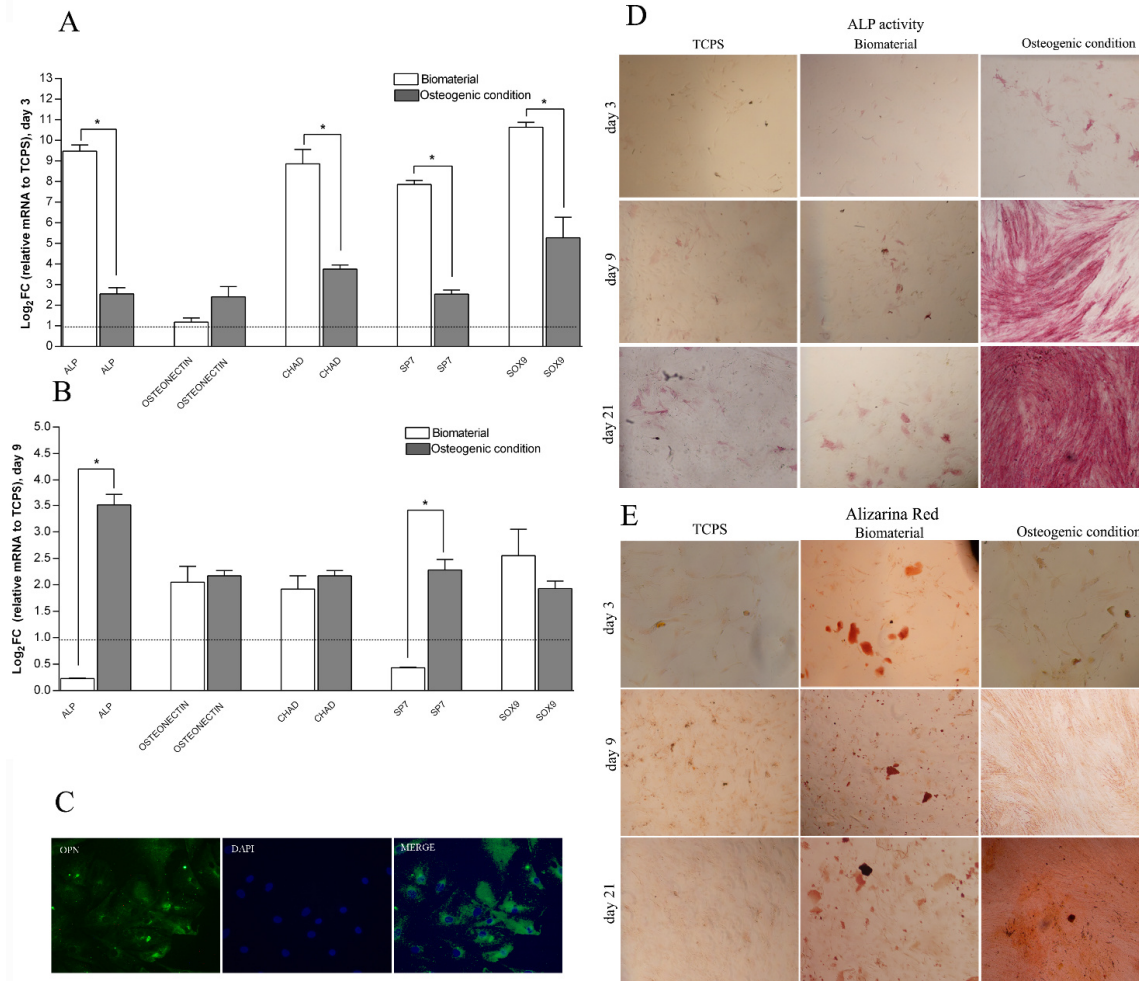
Gene expression of human ECM and adhesion molecules



Genes up-regulated from biomaterial and osteogenic condition at 21 and 40 days	
1	BMP1
2	BMP2
3	BMPR1B
4	CSF2
5	CSF3
6	FGFR2
7	IGF1R
8	ITGA2
9	NOG
10	RUNX2
11	SOX9
12	SP7
13	SPP1
14	TGFB1
15	TNFSF11
16	TWIST1

PCR array analyses of ECM and adhesion molecule genes. Expression of genes was evaluated on hASCs that were grown on Coll/Pro Osteon200 compared with TCPS. A) Regulated genes at d 3. Expression of ITGAM, ITGA3, LAMA2, ITGB5, COL6A2, SELE, COL6A1, and SPP1 genes was up-regulated at d 3, whereas expression of CDH1, KAL1, and CLEC3B genes was downregulated. B) Regulated genes at d 9. Expression of CLEC3B and LAMB3 genes was up-regulated, whereas expression of LAMA3, NTN1, ITGA2, and MMP3 genes was down-regulated.

Osteogenic markers



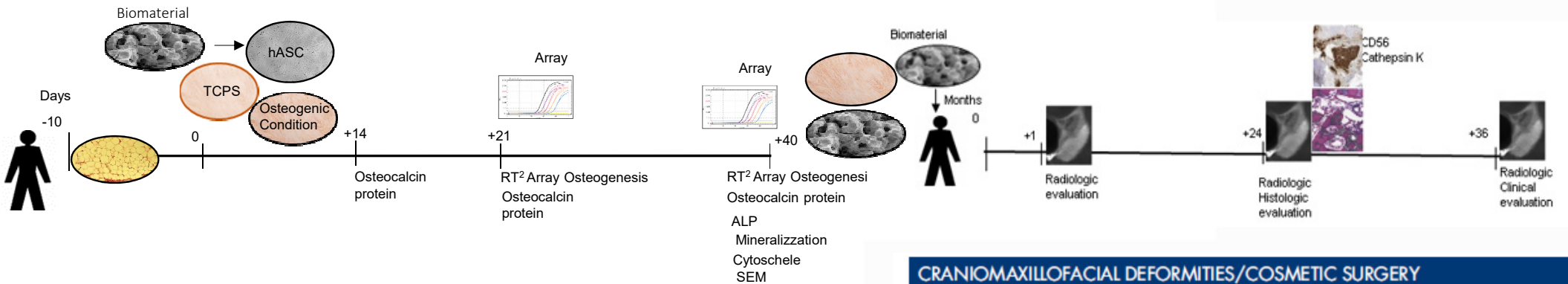
Osteoinductive effect of the Coll/ Pro Osteon200 scaffold on hASCs. Gene expression in hASCs that were grown on Coll/Pro Osteon200 scaffold and osteogenic condition for d 3 and 9. A) Graphical representation of relative gene expression at d 3 using hASCs in basal medium as control group. Quantitative RT-PCR was performed for mRNA of ALP, osteonectin, CHAD, transcription factor osterix (SP7), and transcription factor SRY-box 9 (SOX9). B) Graphical representation of relative gene expression at d 9. C) Immunostaining with Ab against osteopontin protein (OPN) at d 9. D, E) Matrix mineralization (D) and ALP activity of hASCs that were grown on TCPS (E) on scaffold and in OM during 3 temporal intervals (d 3, 9, and 21), (X320).



Experimental Design III



B



CRANIOMAXILLOFACIAL DEFORMITIES/COSMETIC SURGERY

Hydroxyapatite/Collagen Composite Is a Reliable Material for Malar Augmentation

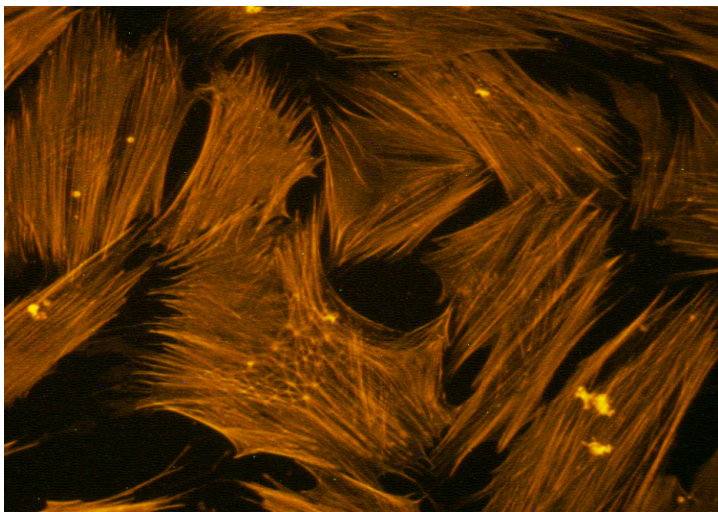
Antonio D'Agostino, MD,* Lorenzo Trevisiol, MD,† Vittorio Favero, MD,‡
 Michael J. Gunson, DDS, MD,§ Federica Pedica, MD,|| Pier Francesco Nocini, MD, DDS,¶
 and G. William Arnett, DDS#

Scaffold: Pro Osteon 200 + Avitene

Pro Osteon
Bone Graft Substitute



Avitene™
Microfibrillar Collagen Hemostat

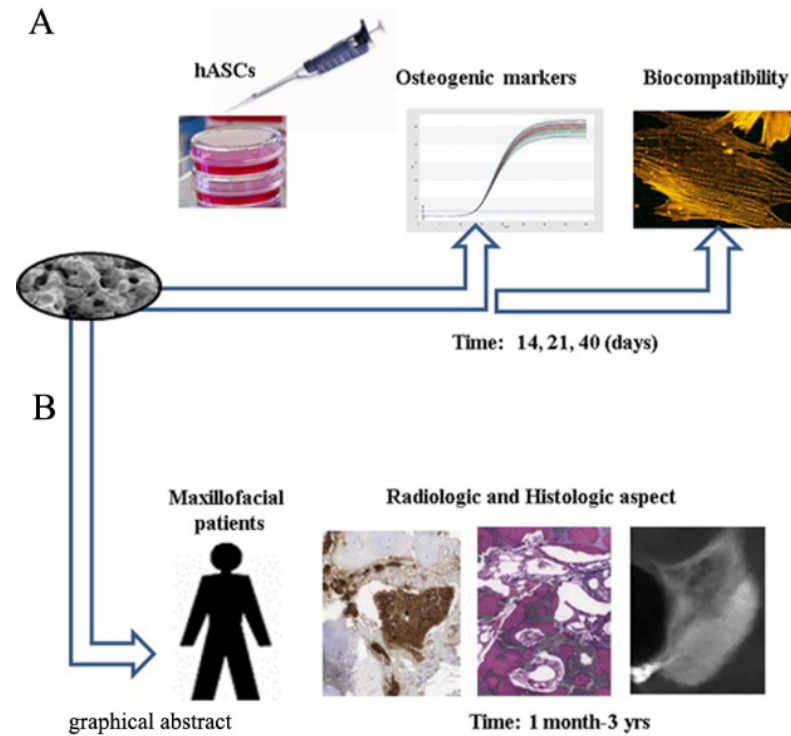


a) Immagine del citoscheletro cellulare delle colture hASC, evidenziato con Phalloidina^{TRITC} dopo 40 gg di co-cultura.

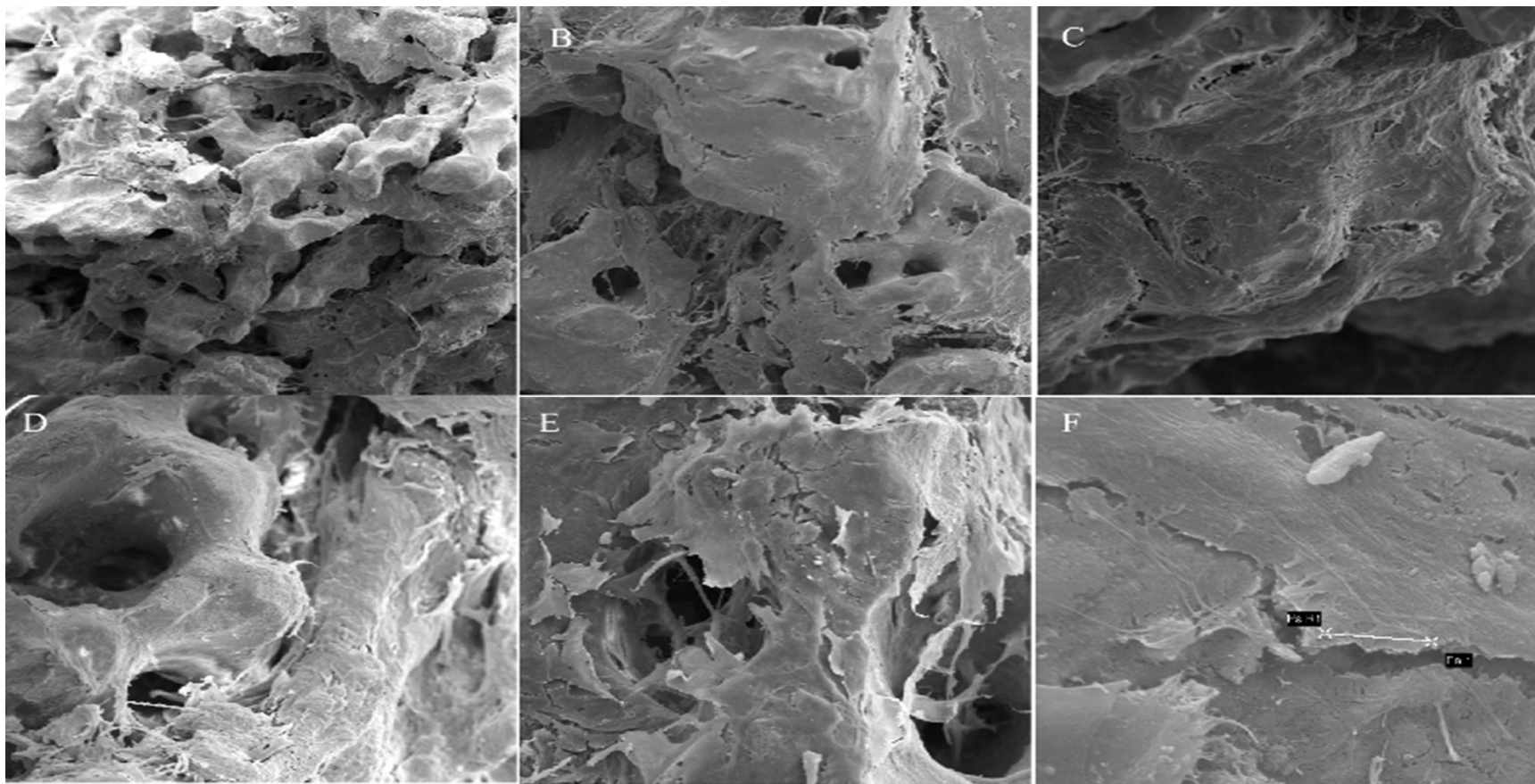
STEM CELLS TRANSLATIONAL MEDICINE™

Hydroxylapatite-collagen hybrid scaffold induces human adipose-derived mesenchymal stem cells (hASCs) to osteogenic differentiation in vitro and bone re-growth in patients. *Stem Cells Transl Medicine.* (2019).

Mazzoni, E., D'Agostino, A., Iaquina, M.R., Bononi, I., Trevisiol, L., Rotondo, J.C., Patergnani, S., Giorgi, C., Gunson, M.J., Arnett, W., Nocini, P.F., Tognon, M., and Martini, F.

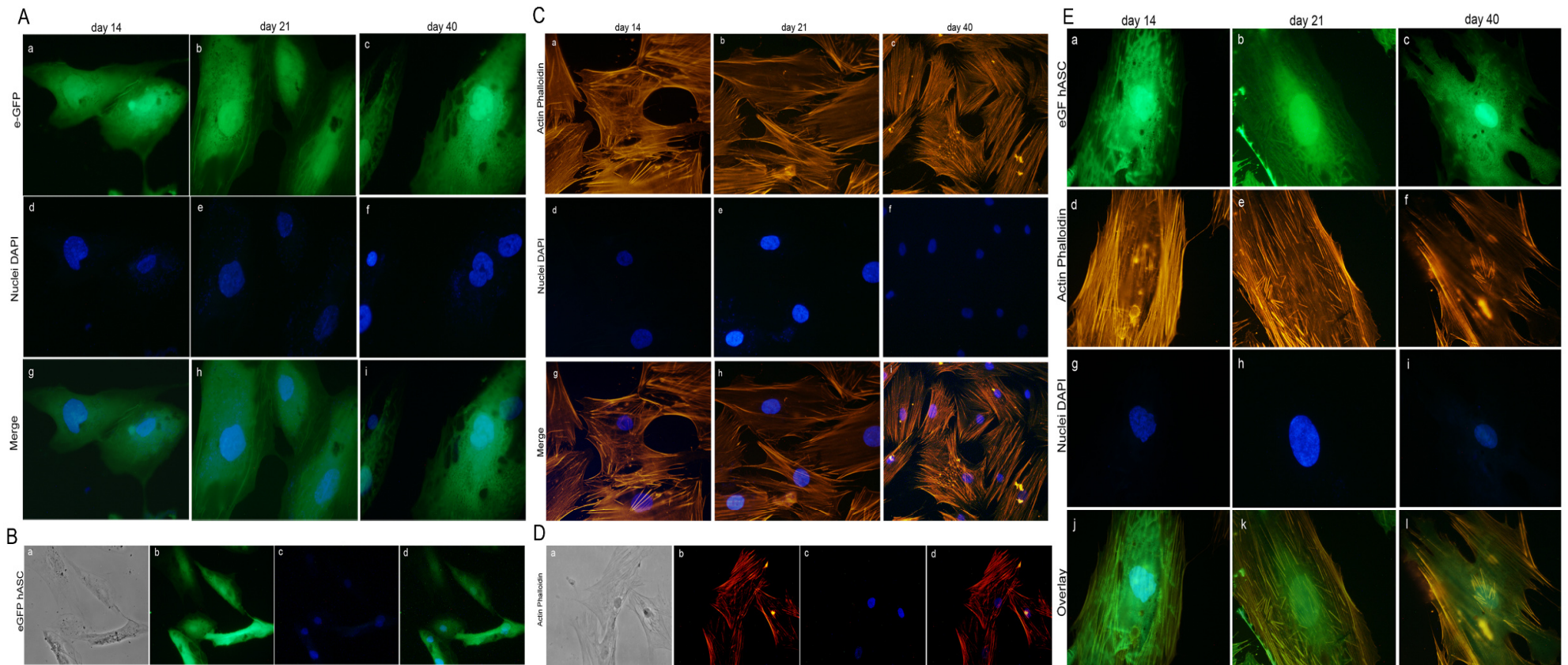


SEM analyses of stem cells and biomaterials (40 days)



SEM analysis of the Coll/HA with hASC at day 40. (A) The scaffold without hASC culture, 86 X magnification. (B-F). hASC grown on HA-derived scaffold until day 40. The structure of scaffold were observed at 133 X (B), 214 X (C), 344 X (D), 647X (E), 6.55KX (F) magnification, respectively.

Cell viability and Cytoskeleton architecture of hASC



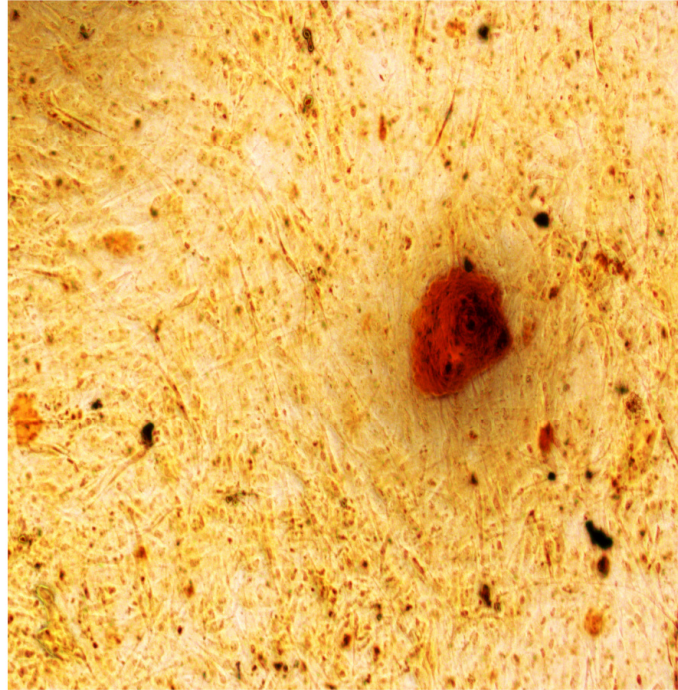
A

Matrix mineralitation

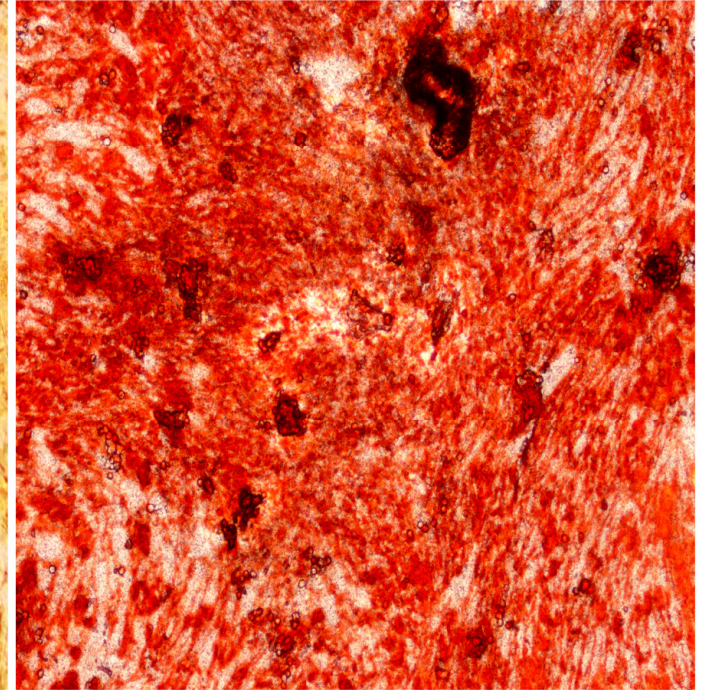
TCPS



Biomaterial



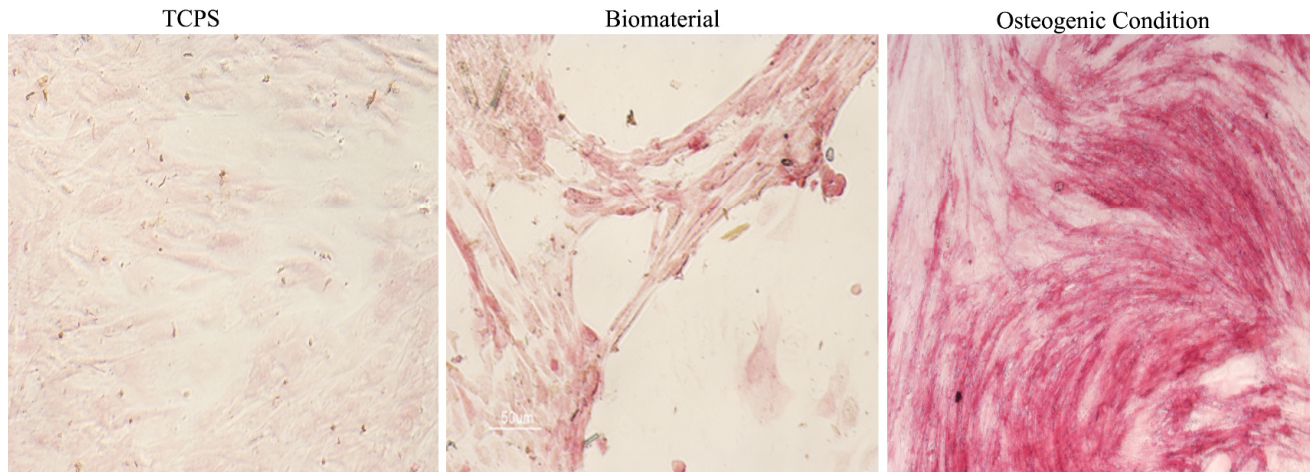
Osteogenic Condition



Osteogenic protein expression: alkaline phosphatase (ALP) activity and CLEC3B at day 40

B

Alkaline Phosphatase Activity

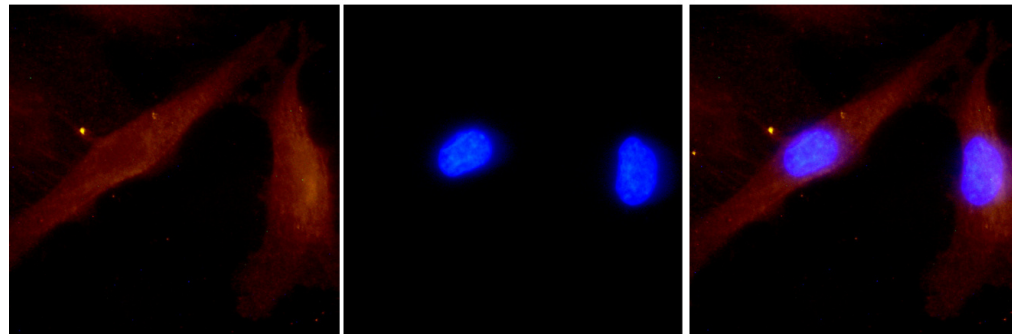


E

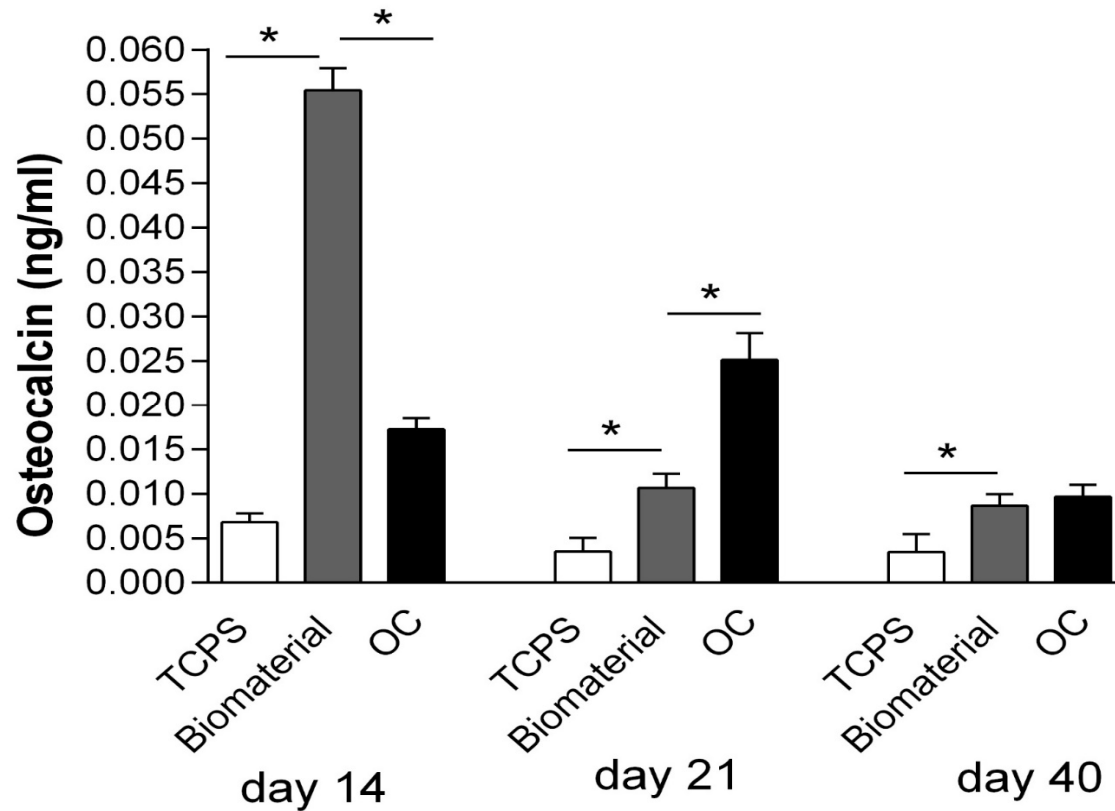
CLEC3B

DAPI

MERGE

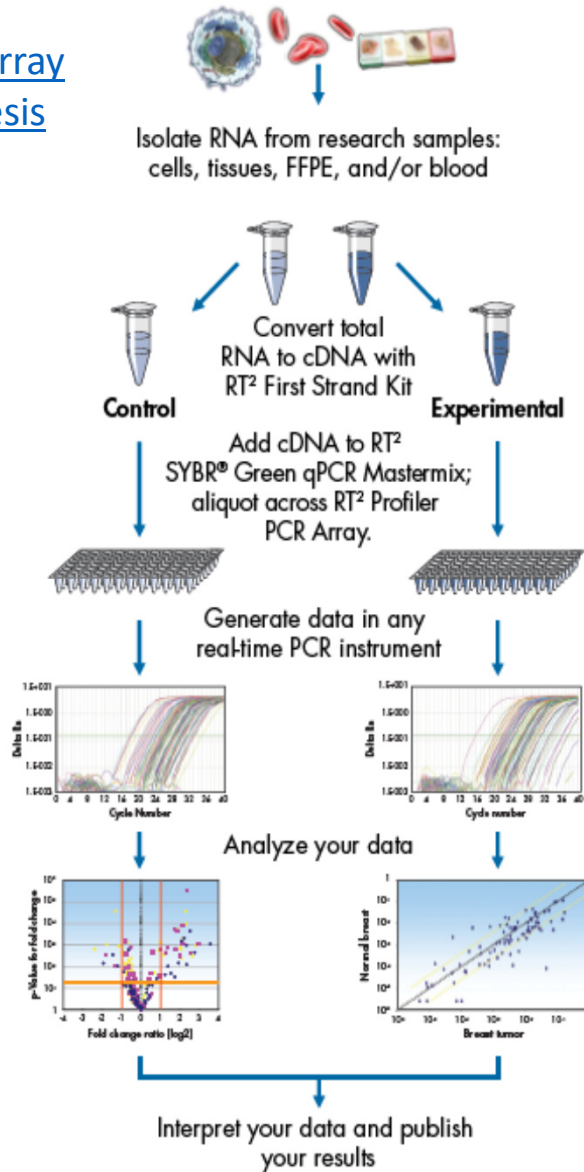


Osteocalcin protein expression



Relative amount of osteocalcin protein in hASC grown on control (TCPS), on the biomaterial and in osteogenic condition (OC). Osteocalcin protein were quantified by enzyme linked immunosorbent assay (ELISA) (eBioscience). A difference between biomaterial and TCPS was observed at day 14, 21 and 40. * $P < 0.0001$. Moreover the biomaterial exhibited the highest relative amount of osteocalcin respect to osteogenic condition at day 14, (Anova and Tukey test).

RT² Profiler™ PCR Array Human Osteogenesis



Skeletal development

Cartilage condensation: BMP1, BMPR1B (ALK6), COL2A1, SOX9.

Ossification: ACVR1 (ALK2), AHSG, BGLAP, BMP1, BMP2, BMP3, BMP4, BMP5, BMP6, BMP7, BMPR1A (ALK3), BMPR1B (ALK6), BMPR2, CDH11, CHRDL1, COL1A1, COL2A1, CSF1 (MCSF), CTSK, DLX5, EGFR (ERBB1), FGF2 (BFGF), FGFR2, GDF10 (BMP3B), GLI1, IGF1, IGF1R, IGF2, IHH, MMP2, MMP8, MMP9, NOG, RUNX2, SMAD1 (MADH1), SMAD3 (MADH3), SOX9, SP7, SPP1, TGFB1, TGFB2, TGFB3, TNFSF11 (RANKL), TWIST1.

Differentiation in osteoclasts: BGLAP, CSF1 (MCSF), TNF, TNFSF11 (RANKL).

Differentiation in osteoblasts: ACVR1 (ALK2), BGLAP, BMP2, BMP4, BMP6, BMP7, DLX5, BMPR1A (ALK3), BMPR1B (ALK6), BMPR2, CHRDL1, COL1A1, FGF2 (BFGF), FGFR2, GDF10 (BMP3B), GLI1, IGF1, IHH, NOG, RUNX2, SMAD1 (MADH1), SMAD3 (MADH3), SP7, SPP1, TWIST1.

Other genes involved in skeletal development: ALPL, COMP, FGFR1, TGFB1 (ALK5), TGFB2.

Bone metabolism

Bone mineralization: ACVR1 (ALK2), AHSG, BGLAP, BMP2, BMP4, BMP6, BMP7, BMPR1A (ALK3), BMPR1B (ALK6), BMPR2, FGFR2, IGF1, SMAD3 (MADH3), SOX9, TGFB1, TGFB3, TWIST1.

Bonding with Ca²⁺ and Homeostasis: ANXA5, BGLAP, CALCR, CDH11, COMP, EGF, FGF2 (BFGF), ITGB1, MMP2, MMP8, TGFB1, VDR.

Molecules of the extracellular matrix (ECM) Collagene: COL10A1, COL14A1, COL15A1, COL1A1, COL1A2, COL2A1, COL3A1, COL5A1.

Extracellular matrix protease inhibitors (ECM): AHSG, SERPINH1 (HSP47).

Proteasi della matrice extracellulare (ECM): CTSK, MMP10, MMP2, MMP8, MMP9, PHEX.

Other molecules adhesion of the extracellular matrix (ECM): ALPL, BGN, FLT1 (VEGFR1).

Molecules of adhesion

Cell-cell adhesion: BMP1, BMPR1B (ALK6), CDH11, COL14A1, COL2A1, EGFR (ERBB1), ICAM1, IHH, ITGB1, SOX9, TGFB1, TNF, TNFSF11 (RANKL), VCAM1.

Molecules adhesion of the extracellular matrix (ECM): CD36, COL3A1, CSF1 (MCSF), ITGA1, ITGA2, ITGA3, ITGAM, ITGB1, SMAD3 (MADH3).

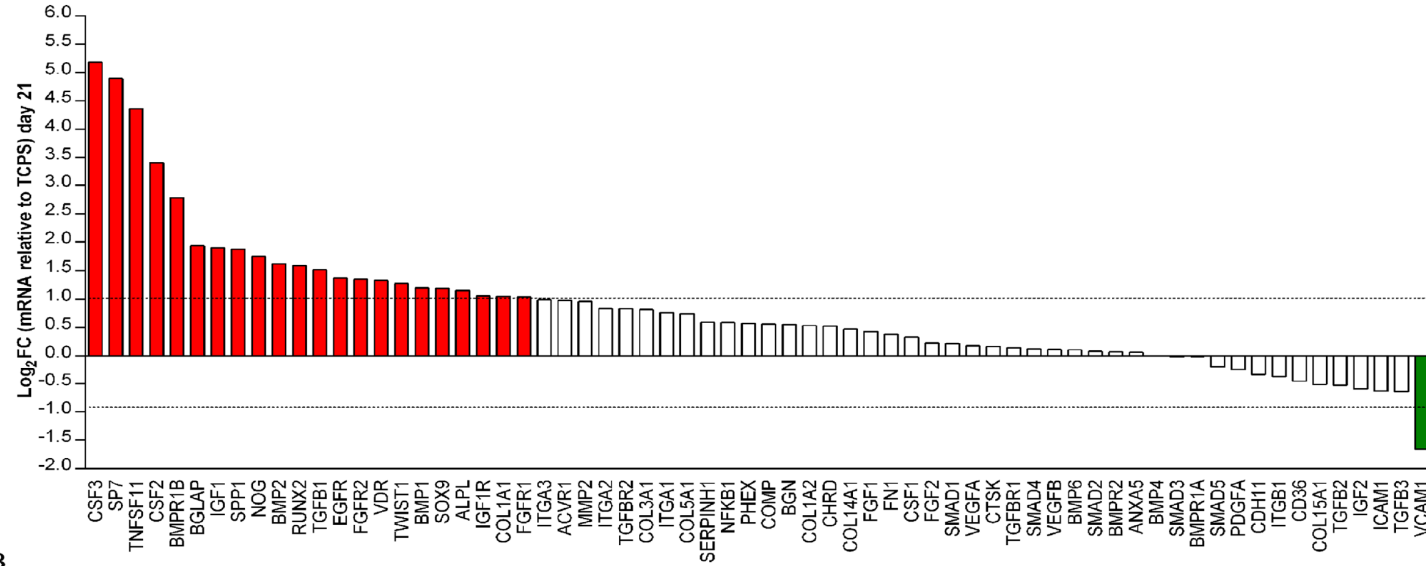
Other molecules adhesion : BGLAP, COL15A1, COL5A1, COMP, FN1, TNF.

Growth factors: CSF2 (GMCSF), CSF3 (GCSF), EGF, FGF1, FGF2 (BFGF), GDF10 (BMP3B), IGF1, IGF2, PDGFA, VEGFA, VEGFB.

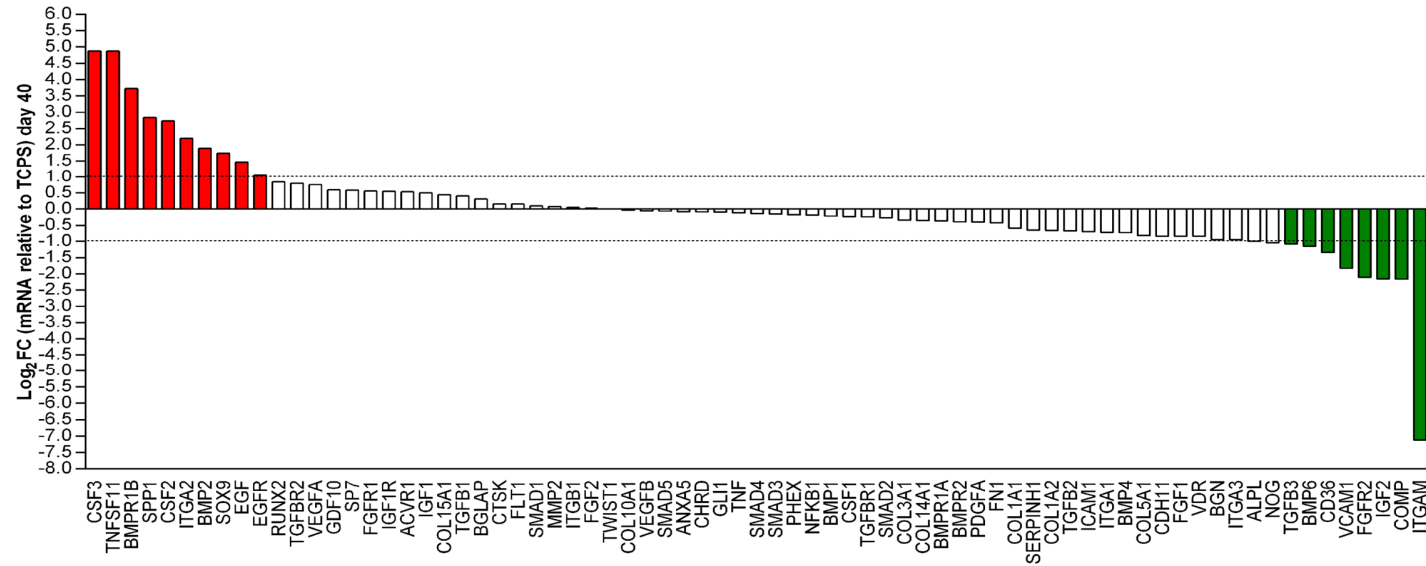
Transcription factors: GLI1, NFKB1, RUNX2, SMAD1 (MADH1), SMAD2 (MADH2), SMAD3 (MADH3), SMAD4 (MADH4), SMAD5 (MADH5), SOX9, TWIST1

Gene expression of osteogenic genes (PCR Array)

A



B



Gene expression of osteogenic genes in hASC cultured on the control (TCPS), biomaterial and in osteogenic condition, quantified by PCR Array. Messenger RNAs (mRNA) of 24 genes implicated in ossification process/pathway, i.e. CSF 2/3, SP7, SPP1, TNFSF11, BMPR1B, BMP1/2, BGLAP, IGF1, NOG, RUNX2, TGFB1, EGFR, FGFR1/2, VDR, TWIST1, SOX9, ALPL, IGF1R, COL1A1, ITGA2, EGF were upregulated compared to the control.

Biomaterial characterization in patients: radiologic and histologic aspect

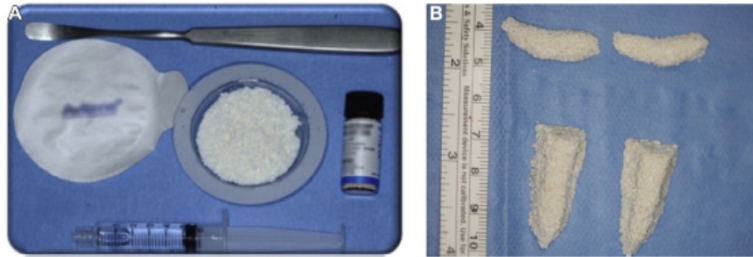
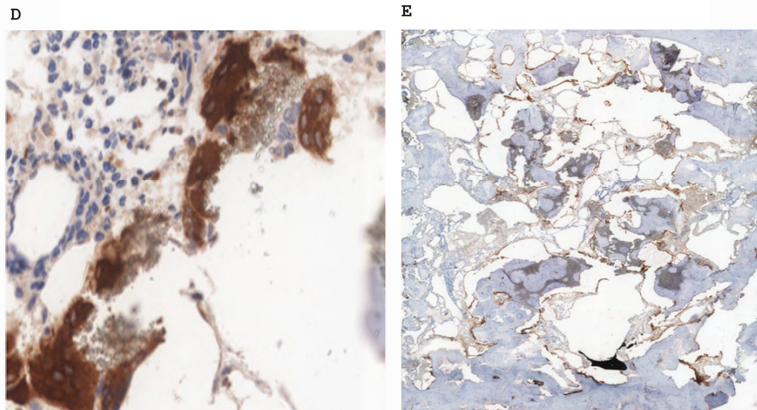


FIGURE 1. A, B, Preparing the prosthesis.

D'Agostino et al. Hydroxyapatite for Maxilar Augmentation. J Oral Maxillofac Surg 2016.



Scaffold characterization in patients: radiologic and histologic aspect. (A-C) Cone-beam tomogram, coronal slice, at t1 (1 month), t2 (24 months) and at t3 (36 months) after surgery. The granular structure is still distinguishable, although less evident, and the partial radiotransparency evolved to a radiopacity similar to that in the compact part of the native bone, making it impossible to distinguish the interface between the prosthesis and bone. The interface between the prosthesis and bone at t3 appears indistinguishable.

(D, E) Biopsy 24 months after implant. Bone maturation gradient can be observed proceeding from the periosteal layer towards the native bone (hematoxylin and eosin stain; magnification X10). (D) **Osteoclasts** surrounding hydroxyapatite residual granules (immunohistochemistry with **cathepsin K**; magnification X20). (E) Higher amount of new bone formation at the layer adjacent to **native bone** (immunohistochemistry with **anti-CD56** antibodies; magnification X20).

CONCLUSIONS

Our in vitro and in vivo data indicate that the innovative hybrid biomaterial satisfies the clinical need for the bone regrowth. Indeed, the osteo-inductivity and osteogenicity proprieties, without negative side effects, were shown.

Grazie e Auguri

